PAPER

Measurement of excitation functions for ^{nat}Cu(α, x) reactions with detailed covariance analysis

IOP Publishing Journal of Physics G: Nuclear and Particle Physics
J. Phys. G: Nucl. Part. Phys. **50** (2023) 015103 (16pp) https://doi.org/10.1088/1361-6471/aca1d7

Measurement of excitation functions for ^{nat}Cu(α, *x*) reactions with detailed covariance analysis

Mahesh Choudhary[1], Aman Sharma[1], A Gandhi[1], Namrata Singh[1], Punit Dubey[1], Mahima Upadhyay[1], Utkarsha Mishra[1], N K Dubey[1], S Dasgupta[2], J Datta[2], K Katovsky[3] and A Kumar[1,*]

[1] Department of Physics, Banaras Hindu University, Varanasi 221005, India
[2] Analytical Chemistry Division, Bhabha Atomic Research Centre, Variable Energy Cyclotron Centre, Kolkata-700064, India
[3] Department of Electrical Power Engineering, Brno University of Technology, Brno-61600, Czech Republic

E-mail: ajaytyagi@bhu.ac.in

Received 27 August 2022, revised 20 October 2022
Accepted for publication 10 November 2022
Published 1 December 2022

Abstract

The excitation functions of ^{66}Ga, ^{67}Ga, ^{65}Zn and ^{64}Cu radioisotopes produced via alpha-induced reaction on ^{nat}Cu were measured using a stacked foil activation method. The gamma-ray activity produced by the above mentioned radionuclides was measured using the HPGe detector. The covariance analysis was performed to quantify the measured cross-section uncertainties as well as the correlation between different alpha energy cross-sections. A covariance matrix and cross-sections for the ^{nat}Cu(α, *x*)^{66}Ga, ^{nat}Cu(α, *x*)^{67}Ga, ^{nat}Cu(α, *x*)^{65}Zn and ^{nat}Cu(α, *x*)^{64}Cu nuclear reactions in the projectile energy range of 15–37 MeV are reported in the present work. The measured reaction cross-sections are compared with the existing experimental data and theoretically simulated results from the TALYS code.

Keywords: excitation functions, covariance analysis, alpha-induced nuclear reactions, statistical nuclear model codes

(Some figures may appear in colour only in the online journal)

* Author to whom correspondence should be addressed.

1. Introduction

Nuclear data on alpha-induced reactions are important for the interpretation of astrophysical observations, nuclear reactors, nuclear medication and radiation therapy [1, 2]. The measurement of alpha-induced nuclear reaction cross-sections on various target materials is useful for the study of nuclear phenomena, the production of medical radioisotopes and nuclear transmutation rates. The ^{nat}Cu is an important target material that produces medical radioisotopes such as ^{66}Ga, ^{67}Ga and ^{64}Cu. The radioisotopes ^{66}Ga, ^{64}Cu are used in the positron emission tomography and ^{67}Ga is also a medical radioisotope which is used in the nuclear medicine for different types of human tumors [3–5]. The experimental nuclear reaction cross-sections of alpha-induced reactions are also important for testing various statistical nuclear model codes and the sensitivity of outcomes to various values of the parameters used for computing the cross-sections [6, 7]. Activation of the target material is a method used to measure reaction cross-sections to produce a radionuclide by detecting the gamma-ray from the radioactive element. This method is widely used in the nuclear reactions involving a variety of projectiles such as alpha, proton, neutrons and photons [8, 9]. In order to determine a reasonable margin that contributes to both safety and nuclear applications, the uncertainty associated with the activation reaction cross-section is very essential. If multiple data points are involved in the measurement of the activation nuclear reaction cross-sections, the correlation between all the data points must also be taken into consideration to prevent the underestimation of the uncertainty in the quantity of interest [10]. Consequently, contemporary evaluations aim to provide the best estimate of not only the cross-section but also uncertainty and covariance, which describe the correlation between estimated cross-sections at different projectile energy range for the same reaction and cross correlation between estimated cross-sections at the same projectile energy for different nuclear reactions [11, 12]. In order to provide better documentation on the uncertainties of the quantities evaluated in each experiment, we need to provide the covariance with the measured cross-section. Evaluators face difficulty in covariance analysis of nuclear reaction cross-section due to very less documentation on correlation and cross correlation study of measured quantity and also evaluators are unable to determine the uncertainty in the measured cross-section. In covariance analysis, we can estimate the uncertainty in the measured quantity using the cross correlation among various attributes [13]. In the present study, we have used natural copper as the target material. With these goals in mind, we have performed an experiment for the alpha-induced reaction on natural copper. Experimental data for these nuclear reactions are available in the exchange format (EXFOR) data repository [14], although none of the data has a complete covariance analysis. Consequently, there is a need for documentation on covariance analysis of these nuclear reactions. In this article, we have presented detailed covariance analysis of reactions ^{nat}Cu(α, x)^{66}Ga, ^{nat}Cu(α, x)^{67}Ga, ^{nat}Cu(α, x)^{65}Zn and ^{nat}Cu(α, x)^{64}Cu, by examining the micro correlations among different variables such as the efficiency of HPGe detector, decay constant, γ-ray counts, incident flux, particle number density and γ-ray intensity. The TALYS nuclear code was used for the theoretical prediction of the above mentioned nuclear reactions [15]. A comparison of the measured nuclear reaction cross-sections with the available experimental data on EXFOR and theoretical prediction from the TALYS nuclear code is also presented.

The present study is divided into the following five sections: section 2 discusses the experimental setup, section 3 discusses the data analysis section, section 4 deals with the results and discussion and section 5 concludes the present work.

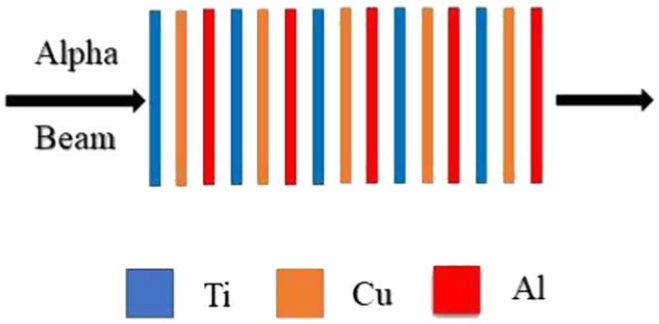

Figure 1. The schematic diagram of Ti-Cu-Al foils arrangement.

Table 1. Description of beam current, radiation time and projectile energy.

Stack number	Incident energy (MeV)	Current (nA)	Irradiation time (h:min)	Energy range (MeV)
1	37	162	5:00	37–23.33
2	32	130	10:35	32–15.90

2. Experimental details

The experiment was performed using the K-130 cyclotron at Variable Energy Cyclotron Center (VECC), Kolkata, India. In the present experiment, the alpha beam was produced by helium gas using the PIG ion source.

The stacked foil activation method [16–19] was used to determine the nuclear reaction cross-sections of alpha-induced reactions on copper in the energy range from the threshold energy of resulting reactions up to 37 MeV. The main advantage of the stacked foil activation method is that we can obtain the whole range of excitation functions using less number of irradiations. In accordance with this method, a stack of the thin target foils i.e. ^{nat}Cu was followed by the ^{nat}Al, which enacted as the catcher foil to capture the recoil radioactive from the target foil. ^{nat}Al (catcher foil) has low *Z*-material which reduces the gamma attenuation during the measurement and does not produce any radioactive in the incident energy range. We have used ^{nat}Ti foil as monitor foil. We ensured monitor foil (^{nat}Ti) before every target foil (^{nat}Cu) to calculate incident flux on target foils. We arranged the stack as ^{nat}Ti ($10 \times 10\,mm^2$) followed by ^{nat}Cu ($10 \times 10\,mm^2$) accompanied by ^{nat}Al ($10 \times 10\,mm^2$). The thickness of ^{nat}Ti, ^{nat}Cu, ^{nat}Al foils were $6.27\,mg\,cm^{-2}$, $13.50\,mg\,cm^{-2}$ and $1.80\,mg\,cm^{-2}$ respectively. In this experiment, we irradiated two sets of stacks at two different energy ranges to get the continuous excitation function for our desired reactions. Table 1 provides information about the beam current, irradiation time and projectile energy. We employed SRIM-2008 (Stopping and Range of Ions in Matter) code to calculate energy degradation of our sequenced stack [20, 21]. A faraday cup was placed after the stack to measure the beam current falling on the foils. The schematic diagram of the stack foils arrangement and the layout of the experimental setup are shown in figures 1 and 2 respectively.

To measure the γ-ray activity, firstly we irradiated the samples and then the activated samples were moved from the experimental hall to the counting room, and opened the target holder safely. After that, the monitor foils and the target foils were separated. We wrapped the

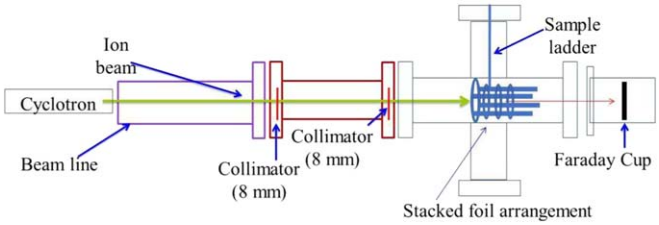

Figure 2. The layout of the experimental setup.

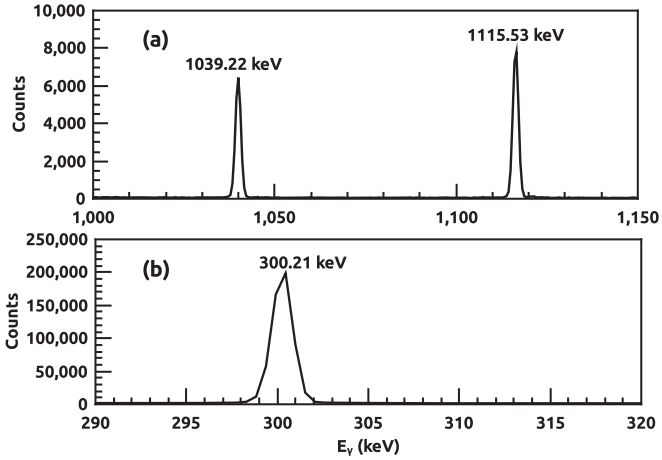

Figure 3. A γ-ray spectrum of the irradiated foil (a) for radionuclide ^{66}Ga (1039.22 keV) and ^{65}Zn (1115.53 keV) (b) for radionuclide ^{67}Ga (300.21 keV).

target and the catcher foil in a small thin polythene bag which was sealed properly to prevent contamination and then placed them on perspex plates for gamma-ray activity counting. Depending on the half-life of the produced radionuclide, we started the counting after various cooling intervals where irradiation stops. We have used a high-purity germanium detector (HPGe) to detect the gamma-ray activity of the samples. The efficiency of the HPGe detector for different gamma energies was calculated by using a ^{152}Eu point source. A γ-ray spectrum of irradiated ^{nat}Cu and ^{nat}Ti foils are shown in figures 3 and 4. In our earlier paper [22], we have provided a detailed explanation of the calibration and efficiency calculations of the HPGe detector as well as its uncertainty and coincidence summing effect.

3. Data analysis

The activation formula, which is given in the following equation, was used to compute the reaction cross-sections for the nuclear reactions ^{nat}Cu(α, x);

$$\sigma = \frac{\lambda e^{\lambda t_c} C_\gamma}{I_\gamma \phi \varepsilon(E_\gamma) N_t (1 - e^{-\lambda t_{\mathrm{irr}}})(1 - e^{-\lambda t_m})}. \tag{1}$$

In this equation, I_γ stands for γ-ray intensity, C_γ for total counts, $\varepsilon(E_\gamma)$ for detector efficiency, ϕ for incident flux, λ for decay constant, and N_t for particle density in the target. The target's irradiation time is represented by the symbol t_{irr}, the target's cooling time is

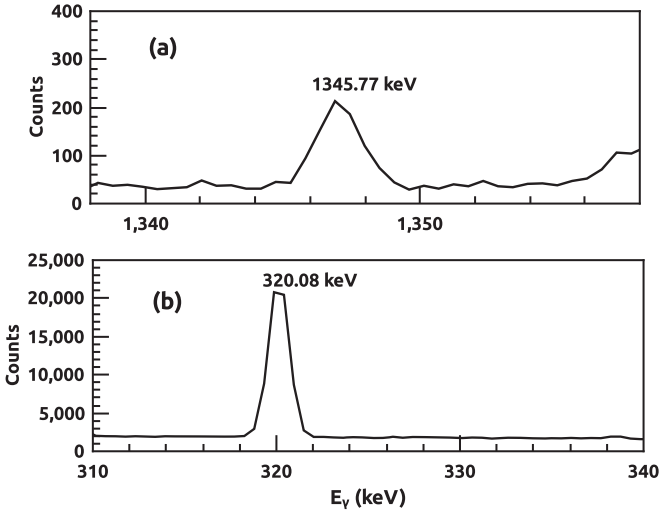

Figure 4. A γ-ray spectrum of the irradiated foil (a) for radionuclide ^{64}Cu (1345.77 keV) (b) for radionuclide ^{51}Cr (320.08 keV).

denoted by t_c, and the sample's counting time is denoted by t_m. When calculating the uncertainty of the measured nuclear reaction cross-section in this study, variables like particle number density in target, detector efficiency, counts, gamma-ray intensity, incident flux and decay constant are taken into consideration. Table 2 provides information about the nuclear reactions, radioactive half-lives, Q-values of the reactions, and decay characteristics. The TALYS nuclear code is used for estimating the cross section of ^{nat}Cu(α, x)^{66}Ga, ^{nat}Cu(α, x)^{67}Ga, ^{nat}Cu(α, x)^{65}Zn and ^{nat}Cu(α, x)^{64}Cu nuclear reactions over the alpha energy range for reaction threshold to 35 MeV.

The TALYS code is based on the Hauser–Fesbach statistical model, which generates the nuclear data for all open reaction channels, on user-defined energy and angle grid [23, 24]. This nuclear code has been used to calculate many physical observables related to nuclear reactions analysis and estimation of reaction cross se-tion. All the input parameters required to calculate the cross section such as—nuclear masses, discrete levels, optical model parameters, level densities, decay schemes, γ-ray strength functions are taken into consideration during optimization in TALYS. We can simulate reactions that have photons, deuterons, ^{3}He, neutrons, protons and tritons particles as an incident particle for target nuclides of mass 12 and heavier energy ranging from 1 keV to 200 MeV. We have used different level density models for theoretical prediction in the TALYS code [25–30]. The outcome of the theoretical calculations for all the reactions are documented in the following section, along with the present measured cross-sections and existing cross-sections data from the EXFOR database. The EXFOR is the library and format for collecting, storing, exchanging and retrieving experimental nuclear reaction data [31].

In Covariance analysis, the uncertainty propagation can be explained using the cross correlation between several observed values [32, 33]. The method we have used to calculate the covariance matrix of the nuclear reaction in the present work is given in our previous article [22, 34]. In the present experiment, we have used ^{nat}Ti(α, x)^{51}Cr nuclear reaction as a monitor reaction. The monitor reaction cross-sections were used to calculate the flux for the natural copper reaction cross-sections. The flux for natural copper reaction cross-sections was measured by using the monitor foils and hence the uncertainty associated with flux is

Table 2. Nuclear reactions and other parameters of the radionuclides generated by ^{nat}Zn(α, x) reactions and investigated in the present work.

Radionuclide	Half-life ($t_{1/2}$)	Decay mode (%)	E_γ (keV)	I_γ (%)	Reaction	Q-value (MeV)
^{66}Ga	9.49 ± 0.03 h	$ec + \beta^+$(100)	1039.22	37 ± 2	^{63}Cu(α, n)	−7.50
					^{65}Cu(α, 3n)	−25.33
^{67}Ga	3.26 ± 0.0005 d	ec (100)	300.21	16.64 ± 0.12	^{63}Cu(α, γ)	3.72
					^{65}Cu(α, 2n)	−14.10
^{65}Zn	243.93 ± 0.09 d	$ec + \beta^+$(100)	1115.53	50.04 ± 0.10	^{63}Cu(α,d)	−10.38
					^{63}Cu(α, n+p)	−12.60
					^{65}Cu(α, n+t)	−21.95
					^{65}Cu(α, 2n+d)	−28.21
					^{65}Cu(α, 3n+p)	−30.43
^{64}Cu	12.70 ± 0.0002 h	$ec + \beta^+$(61.5) β^-(38.5)	1345.77	0.472 ± 0.0004	^{63}Cu(α,^{3}*He*)	−12.66
					^{65}Cu(α, n+α)	−9.91

Table 3. The correlations among the different attributes.

Attributes	Correlation
Flux (ϕ)	0
Counts (C)	0
Decay Constant (λ)	1
γ-ray Intensity (I_γ)	1
Number Density (N_t)	1
Detector Efficiency $\epsilon(E_\gamma)$	1

Table 4. The uncertainty in decay constant ($\Delta\lambda$), efficiency ($\Delta\epsilon$), counts (ΔC_γ), and gamma-ray intensity (ΔI_γ).

Reactions	$\Delta\lambda$ (%)	$\Delta\epsilon$ (%))	ΔC_γ (%)	ΔI_γ (%)
^{nat}Cu(α, x)^{66}Ga	0.31	1.27	1–3	0.54
^{nat}Cu(α, x)^{67}Ga	0.02	1.56	1–2	0.01
^{nat}Cu(α, x)^{65}Zn	0.04	1.55	1–3	0.002
^{nat}Gu(α, x)^{64}Cu	0.0004	2.27	3–8	0.08

measured by taking care of the uncertainty in the number of counts of 320.08 keV gamma-ray, particle number density in monitor foil as well as detector efficiency. The gamma-ray of 320.08 keV rises from the decay of ^{51}Cr radionuclide. The uncertainty in the flux was 4%. In this work, the uncertainty in decay constant ($\Delta\lambda$) was calculated according to the following equation [33];

$$\Delta\lambda = \frac{\ln(2)\Delta T_{1/2}}{T_{1/2}^2}, \tag{2}$$

where, $\Delta T_{1/2}$ is the uncertainty in the half-life of radionuclides and $T_{1/2}$ is the half-life of the radionuclides. The $\Delta T_{1/2}$ and $T_{1/2}$ were taken from evaluated nuclear structure data file (ENSDF). The uncertainty propagation in efficiency of detector ($\Delta\epsilon$) was done by considering different attributes such as uncertainties in counts of particular gamma-ray of standard ^{152}Eu point source (ΔC), uncertainties in gamma-ray intensity (ΔI_γ), uncertainties in the known activity of standard ^{152}Eu point source (ΔA_O), uncertainties in decay constant ($\Delta\lambda$) of ^{152}Eu. The number of particles inside the target was calculated by the following formula:

$$N_t = \frac{WN_a}{M}, \tag{3}$$

where W is the weight of the target foil, M is the mass number of target material and Na is the Avogadro number. The uncertainty in the number of particles in the target foil was propagated from the uncertainty in the weight of the target foil. To calculate the net counts of a gamma peak, we subtract the background count from the total number of the gamma peak. So, the uncertainty in the gamma peak area was calculated from the square root of the total number of counts and the background counts. The uncertainty in the γ-ray intensity (ΔI_γ) was taken from the ENSDF.

The correlations among the variables we take into account in this work are given in table 3. The uncertainty in the particles density in the target material (ΔN_t) was 0.06%. In table 4,

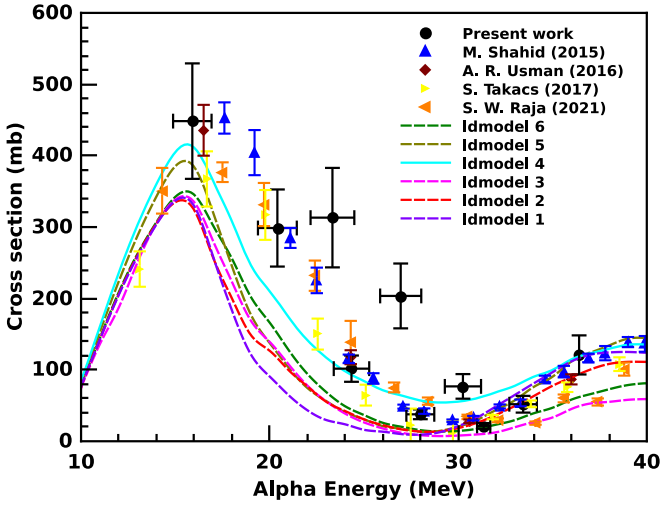

Figure 5. Cross sections for ^{nat}Cu(α, x)^{66}Ga reaction from this study in comparison to the available experimental data from EXFOR and theoretical calculation from TALYS.

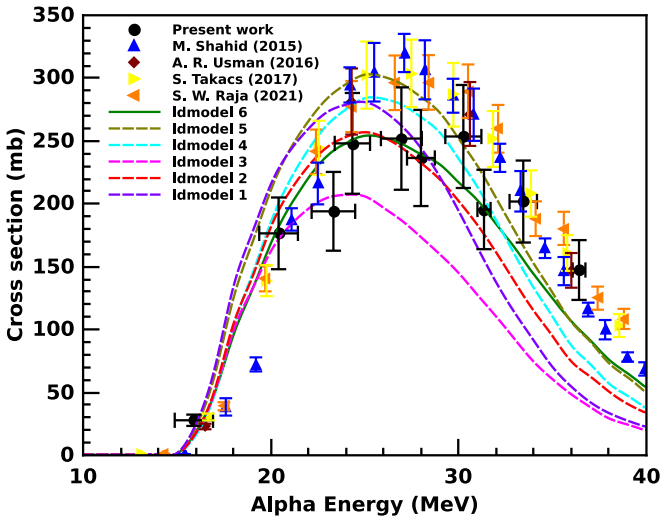

Figure 6. Cross sections for ^{nat}Cu(α, x)^{67}Ga reaction from this study in comparison of the available experimental data from EXFOR and theoretical calculation from TALYS.

percentage uncertainties of decay constant ($\Delta\lambda$), detector's efficiency ($\Delta\epsilon$), counts (ΔC) and γ-ray intensity (ΔI_γ) are listed. Figures 5–8 show the estimated spread in the incident alpha beam energy for each energy point.

4. Results and discussion

In this section, the reaction cross-section uncertainty and a covariance matrix of ^{nat}Cu(α, x) reaction have been described from threshold energy to 37 MeV for individual nuclear reactions. In this study, the obtained nuclear reaction cross-sections were compared with the experimental data taken from EXFOR and also with the predicted theoretical results from the

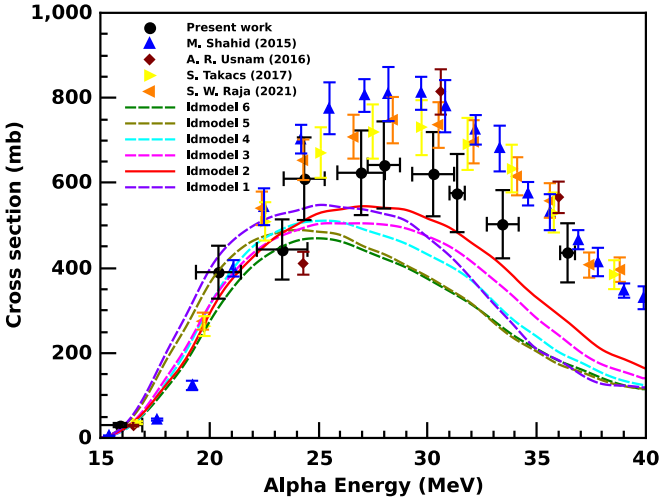

Figure 7. Cross sections for ^{nat}Cu(α, x)^{65}Zn reaction from this study in comparison of the available experimental data from EXFOR and theoretical calculation from TALYS.

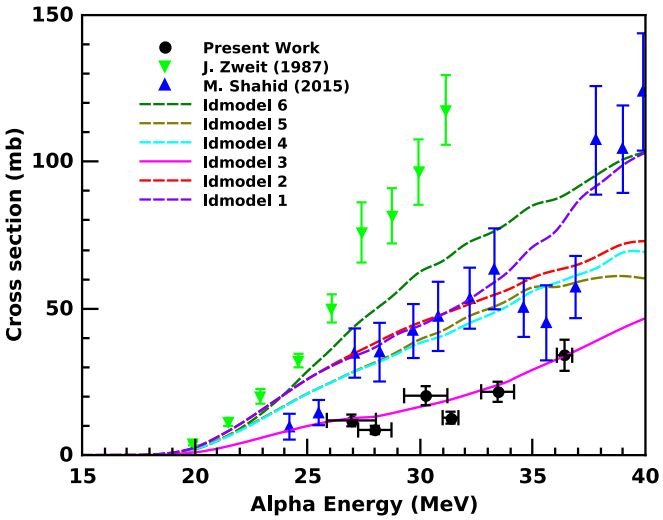

Figure 8. Cross sections for ^{nat}Cu(α, x)^{64}Cu reaction from this study in comparison of the available experimental data from EXFOR and theoretical calculation from TALYS.

TALYS nuclear code. The measured reaction cross-sections with their covariance matrix are given in tables 5–8 and the excitation function of these nuclear reactions are shown in figures 5–8.

4.1. The ^{nat}Cu(α, x)^{66}Ga reaction

In the present work, the computed cross-section values for the ^{nat}Cu(α, x)^{66}Ga nuclear reaction are shown in figure 5 together with the theoretical excitation curve from the TALYS nuclear code and previously estimated cross-sections available on the EXFOR data library. A

γ-ray of energy 1039.22 keV with an intensity of 37% that decays from the ^{66}Ga radioisotope was used to determine the nuclear reaction cross-sections for ^{nat}Cu(α, x)^{66}Ga. The 1039.22 keV γ-ray measurement from the HPGe detector was started after a cooling time of 57 h from the end of bombardment. It can be observed from figure 5, that the measured experimental results overestimate the theoretical result of the ldmodel 4 in the projectile energy range between 15 and 30 MeV and above 30 MeV the theoretical result of the ldmodel 4 agrees with the measured reaction cross-section. The obtained experimental results in this study for ^{nat}Cu(α, x)^{66}Ga nuclear reaction are consistent with the existing reaction data reported by Raja *et al*, Takacs *et al*, Usman *et al* and Shahid *et al* [35–38] as presented in figure 5. In table 5, the reaction cross-sections obtained for the nuclear reaction ^{nat}Cu(α, x)^{66}Ga are listed along with their uncertainties as well as covariance matrix.

4.2. The ^{nat}Cu(α, x)^{67}Ga reaction

In the present work, the computed cross-section values for the ^{nat}Cu(α, x)^{67}Ga nuclear reaction are shown in figure 6 together with the theoretical excitation curve from the TALYS nuclear code and previously estimated cross-sections available on the EXFOR data library. A γ-ray of energy 300.21 keV with an intensity of 16.64% that decays from the ^{67}Ga radioisotope was used to determine the nuclear reaction cross-sections for ^{nat}Cu(α, x)^{67}Ga. The 300.21 keV γ-ray measurement from the HPGe detector was started after a cooling time of 11.54 d from the end of bombardment. As we can see from figure 6, the theoretical result of the ldmodel 6 agrees with the calculated reaction cross-section in the projectile energy range between 15 and 37 MeV. The obtained experimental results in this study for ^{nat}Cu(α, x)^{67}Ga nuclear reaction are consistent with the existing reaction data reported by Raja *et al*, Takacs *et al*, Usman *et al* and Shahid *et al* [35–38] as presented in figure 6. In table 6, the reaction cross-sections obtained for the nuclear reaction ^{nat}Cu(α, x)^{67}Ga are listed along with their uncertainties as well as covariance matrix.

4.3. The ^{nat}Cu(α, x)^{65}Zn reaction

In the present work, the computed cross-section values for the ^{nat}Cu(α, x)^{65}Zn nuclear reaction are shown in figure 7 together with the theoretical excitation curve from the TALYS nuclear code and previously estimated cross-sections available on the EXFOR data library. A γ-ray of energy 1115.53 keV with an intensity of 50.04% that decays from the ^{65}Zn radioisotope was used to determine the nuclear reaction cross-sections for ^{nat}Cu(α, x)^{65}Zn. The 1115.53 keV γ-ray measurement from the HPGe detector was started after a cooling time of 37.34 d from end of bombardment. As we can see from figure 7, the theoretical results of ldmodel 2 are slightly lower than the measured experimental results. The obtained experimental results in this study for ^{nat}Cu(α, x)^{65}Zn nuclear reaction are consistent with existing reaction data reported by Raja *et al*, Takacs *et al*, Usman *et al* and Shahid *et al* [35–38] as presented in figure 7. In table 7, the reaction cross-sections obtained for the nuclear reaction ^{nat}Cu(α, x)^{65}Zn are listed along with their uncertainties as well as covariance matrix.

4.4. The ^{nat}Cu(α, x)^{64}Cu reaction

In the present work, the computed cross-section values for the ^{nat}Cu(α, x)^{64}Cu nuclear reaction are shown in figure 8 together with the theoretical excitation curve from the TALYS nuclear code and previously estimated cross-sections available on the EXFOR data library. A γ-ray of energy 1345.77 keV with an intensity of 0.74% that decays from the ^{64}Cu radioisotope was used to determine the nuclear reaction cross-sections for ^{nat}Cu(α, x)^{64}Cu. The

Table 5. The measured cross-sections for ^{nat}Cu(α, x)^{66}Ga reaction from this study with uncertainties and covariance matrix.

E_α (MeV)	Cross-section (mb) ($\sigma \pm \triangle\sigma$)	Covariance matrix									
15.90 ± 1.02	448.42 ± 80.87	6541.0									
20.41 ± 1.03	298.68 ± 54.0	4100.0	2916.5								
23.33 ± 1.16	313.22 ± 69.66	5223.9	3491.9	4853.6							
24.34 ± 0.94	101.69 ± 18.40	1400.7	935.5	1193.8	338.8						
26.95 ± 1.09	203.55 ± 45.41	3405.3	2276.3	3050.0	778.2	2062.3					
27.99 ± 0.74	37.72 ± 6.83	521.2	348.1	444.6	118.9	289.8	46.7				
30.25 ± 0.96	76.84 ± 17.23	1289.1	861.7	1155.8	294.6	753.8	109.7	297.1			
31.35 ± 0.35	21.51 ± 3.91	298.1	199.1	254.5	68.0	165.9	25.3	62.8	15.3		
33.44 ± 0.73	51.86 ± 11.72	872.6	583.3	782.9	199.4	510.6	74.2	193.5	42.5	137.5	
36.41 ± 0.34	120.91 ± 27.38	2040.5	1363.0	1831.8	466.3	1194.8	173.6	452.8	99.4	306.7	750.0

Table 6. The measured cross-sections for ^{nat}Cu(α, x)^{67}Ga reaction from this study with uncertainties and covariance matrix.

E_α (MeV)	Cross-section (mb) ($\sigma \pm \triangle\sigma$)	Covariance matrix									
15.90 ± 1.02	27.86 ± 4.50	20.2									
20.41 ± 1.03	176.53 ± 28.53	120.5	814.3								
23.33 ± 1.16	194.06 ± 31.33	132.3	838.4	981.6							
24.34 ± 0.94	248.10 ± 40.08	169.2	1072.8	1177.7	1607.1						
26.95 ± 1.09	251.93 ± 40.73	171.9	1089.9	1199.6	1531.1	1659.4					
27.99 ± 0.74	326.49 ± 38.25	161.4	1096.4	1203.7	1540.3	1564.9	1468.8				
30.25 ± 0.96	253.58 ± 40.97	173.0	1096.4	1203.7	1540.3	1564.9	1468.8	1678.7			
31.35 ± 0.35	195.52 ± 31.59	133.3	844.8	927.5	1186.9	1205.8	1131.8	1213.0	997.9		
33.44 ± 0.73	201.84 ± 32.61	137.6	872.4	957.8	1225.6	1245.2	1168.7	1252.6	965.2	1063.6	
36.41 ± 0.34	147.37 ± 23.79	100.4	636.6	698.9	894.3	908.6	852.8	914.1	704.3	727.3	566.2

Table 7. The measured cross-sections for ^{nat}Cu(α, x)^{65}Zn reaction from this study with uncertainties and covariance matrix.

E_α (MeV)	Cross-section (mb) ($\sigma \pm \triangle\sigma$)	Covariance matrix									
15.90 ± 1.02	30.33 ± 4.86	23.6									
20.41 ± 1.03	389.95 ± 62.25	281.8	3874.9								
23.33 ± 1.16	443.37 ± 70.78	320.3	4124.8	5009.4							
24.34 ± 0.94	609.78 ± 96.16	439.98	5664.9	6438.0	9440.1						
26.95 ± 1.09	623.81 ± 99.52	450.74	5800.0	6591.5	9052.6	9905.2					
27.99 ± 0.74	642.15 ± 102.45	463.7	5971.1	6786.0	9319.7	9541.9	10 495.0				
30.25 ± 0.96	620.52 ± 99.08	448.3	5772.9	6560.7	9010.4	9225.1	9497.3	9816.7			
31.35 ± 0.35	576.06 ± 91.93	416.2	5358.7	6090.0	8363.9	8563.2	8815.9	8523.2	8451.2		
33.44 ± 0.73	502.79 ± 80.20	363.0	4674.2	5312.1	7295.5	7469.4	7689.8	7434.5	6901.1	6432.4	
36.41 ± 0.34	435.47 ± 69.56	314.7	4052.7	4605.8	6325.6	6476.3	6667.4	6446.1	5983.6	5219.3	4838.3

Table 8. The measured cross-sections for ^{nat}Cu(α, x)^{64}Cu reaction from this study with uncertainties and covariance matrix.

E_α (MeV)	Cross-section (mb) ($\sigma \pm \triangle\sigma$)	Covariance matrix					
26.95 ± 1.09	11.83 ± 2.0	3.99					
27.99 ± 0.74	8.59 ± 1.44	2.14	1.99				
30.25 ± 0.96	20.26 ± 3.25	5.05	3.66	10.53			
31.35 ± 0.35	12.77 ± 2.03	3.18	2.31	5.45	4.13		
33.44 ± 0.73	21.59 ± 3.43	5.39	3.91	9.22	5.80	11.76	
36.41 ± 0.34	34.04 ± 5.30	8.51	6.17	14.56	9.17	15.52	28.08

1345.77 keV γ-ray measurement from the HPGe detector was started after a cooling time of 57 h from end of bombardment. As we can see from figure 8, the theoretical result of the ldmodel 3 agrees with the calculated reaction cross-section. The obtained experimental results in this study for ^{nat}Cu(α, x)^{64}Cu nuclear reaction are lower than existing reaction data reported by Shahid *et al* and Zweit *et al* [38, 39] as presented in figure 8. In table 8, the reaction cross-sections obtained for the nuclear reaction ^{nat}Cu(α, x)^{64}Cu are listed along with their uncertainties as well as covariance matrix.

5. Conclusion

In the present work, the stack foil activation method was used to determine the nuclear reaction cross-section in the projectile energy range 15–37 MeV for ^{nat}Cu(α, x)^{66}Ga, ^{nat}Cu(α, x)^{67}Ga, ^{nat}Cu(α, x)^{65}Zn and ^{nat}Cu(α, x)^{64}Cu reactions and for the first time the covariance analysis was used to calculate the uncertainty of the measured cross-sections for the above mentioned nuclear reactions. The excitation function of ^{nat}Cu(α, x)^{66}Ga, ^{nat}Cu(α, x)^{67}Ga and ^{nat}Cu(α, x)^{65}Zn nuclear reactions presented in this investigation are in good agreement with the existing reaction data from EXFOR, but excitation function of ^{nat}Cu(α, x)^{64}Cu nuclear reaction in this study is lower than the existing reaction data from EXFOR. We obtained the best theoretical results using ldmodel 4 for nuclear reactions ^{nat}Cu(α, x)^{66}Ga, ldmodel 6 for nuclear reaction ^{nat}Cu(α, x)^{67}Ga, ldmodel 3 for nuclear reaction ^{nat}Cu(α, x)^{64}Cu and ldmodel-2 for nuclear reaction ^{nat}Cu(α, x)^{65}Zn. The measured nuclear reactions presented in this study are used as monitor reactions for alpha-induced reactions on different target therefore accuracy and precision of the measurements was the primary goal of this study because previous work by Raja *et al*, Takacs *et al*, Usman *et al*, Shahid *et al* and Zweit *et al* [35–39] did not address various types of corrections and covariance analysis related to the experimental data.

Acknowledgments

The author (Mahesh Choudhary) is thankful for financial support in the form of Senior Research Fellowships from the Council of Scientific and Industrial Research (CSIR), Government of India, (File No 09/013(882)/2019-EMR-1). The SERB, DST, Government of India [Grant No. CRG/2019/000360], IUAC-UGC, Government of India (Sanction No. IUAC/XIII.7/UFR- 71 353) and Institutions of Eminence (IoE) BHU [Grant No. 6031] are also gratefully acknowledged by one of the author (A Kumar).

We acknowledge the kind support provided by Prof Chandana Bhattacharya, Head, Experimental Nuclear Physics Division, VECC, Kolkata and Prof AK Tyagi, Director, Chemistry Group, BARC, Mumbai towards the successful execution of the experiment. We would also like to express our gratitude to VECC's Cyclotron (K-130) staff for providing us with high-quality beams throughout the experiment.

Data availability statement

All data that support the findings of this study are included within the article (and any supplementary files).

ORCID iDs

Mahesh Choudhary https://orcid.org/0000-0002-4522-5436
Aman Sharma https://orcid.org/0000-0001-6444-512X
A Gandhi https://orcid.org/0000-0001-8372-663X

References

[1] Korkulu Z *et al* 2018 *Phys. Rev.* C **97** 045803
[2] Qaim S M, Spahn I, Scholten B and Neumaier B 2016 *Radiochim. Acta* **104** 601–24
[3] Avagyan R, Avetisyan R, Bazoyan G, Hakobyan M and Kerobyan I 2014 *Universal J. Appl.Sci.* **2** 221–4
[4] D Kim J Y *et al* 2009 *Appl. Radiat. Isot.* **67** 1190–4
[5] E Graham M C, Pentlow K S, Mawlawi O, Finn R D, Daghighian F and Larson S M 1997 *Med. Phys.* **24** 317–26
[6] Kiss G G *et al* 2018 *Phys. Rev.* C **97** 055803
[7] Amjed N, Naz A, Wajid A M, Aslam M N and Ahmad I 2022 *Appl. Radiat. Isot.* **188** 110379
[8] Glascock M D and Neff H 2003 *Meas. Sci. Technol.* **14** 1516
[9] Ishii K, Valladon M and Debrun J L 1978 *Nucl. Instrum. Methods* **150** 213–9
[10] Smith D L and Otuka N 2012 *Nucl. Data Sheets* **113** 3006
[11] Gandhi A *et al* 2021 *Eur. Phys. J. Plus* **136** 1
[12] Lawriniang B *et al* 2019 *J. Radioanal. Nucl. Chem.* **319** 695
[13] Gandhi A *et al* 2020 *Phys. Rev.* C **102** 014603
[14] Otuka N *et al* 2014 *Nucl. Data Sheets* **120** 272
[15] Koning A J 2008 *Proceedings of the International Conference on Nuclear Data for Science and Technology (Nice, France, April 22–27, 2007)* ed O Bersillon *et al* (EDP Sciences) 211–4
[16] Uddin M S, Kim K S, Nadeem M, Sudar S and Kim G N 2017 *Eur. Phys. J.* A **53** 1–10
[17] Takacs S, Takacs M P, Hermanne A, Tarkanyi F and Rebeles R A 2013 *Nucl. Instrum. Methods Phys. Res.* B **297** 44–57
[18] Takacs S, Takacs M P, Hermanne A, Tarkanyi F and Rebeles R A 2012 *Nucl. Instrum. Methods Phys. Res.* B **278** 93–105
[19] Siiskonen T, Huikari J, Haavisto T, Bergman J, Heselius S J, Lill J O, Lonnroth T and Perajarvi K 2009 *Appl. Radiat. Isot.* **67** 2037–9
[20] Ziegler J F, Biersack J P and Ziegler M D 2018 SRIM-The Stopping and Range of Ions in Matter (SRIM Co., 2008). URL:http://www.SRIM.org
[21] Sigmund P and Schinner A 2017 *Nucl. Instrum. Methods Phys. Res.* B **410** 78–87
[22] Choudhary M *et al* 2022 *Eur. Phys. J.* A **58** 95
[23] Koning A J and Rochman D 2012 *Nucl. Data Sheets* **113** 2841
[24] Sekerci M 2020 *Radiochim. Acta* **108** 459–67
[25] Gilbert A and Cameron A G W 1965 *Can. J. Phys.* **43** 1446–96
[26] Dilg W, Schantl W, Vonach H and Uhl M 1973 *Nucl. Phys.* A **217** 269
[27] Ignatyuk A V, Weil J L, Raman S and Kahane S 1993 *Phys. Rev.* C **47** 1504

[28] Goriely S, Tondeur F and Pearson J M 2001 *At. Data Nucl. Data Tables* **77** 311–81
[29] Goriely S, Hilaire S and Koning A J 2008 *Phys. Rev.* C **78** 064307
[30] Hilaire S, Girod M, Goriely S and Koning A J 2012 *Phys. Rev.*C **86** 064317
[31] IAEA-EXFOR Experimental nuclear reaction database https://www-nds.iaea.org/exfor (Data retrieved on July 2022)
[32] Gandhi A *et al* 2021 *Eur. Phys. J.* A **57** 1
[33] Otuka N 2017 *Radiat. Phys. Chem.* **140** 502–10
[34] Gandhi A *et al* 2022 *Chin. Phys.* C **46** 014002
[35] Raja S W *et al* 2021 *Nucl. Phys.* A **1015** 122309
[36] Takacs S *et al* 2017 *Nucl. Instrum. Methods Phys. Res.* B **397** 33–8
[37] Usman A R *et al* 2016 *Appl. Radiat. Isot.* **114** 104
[38] Shahid M *et al* 2015 *Nucl. Instrum. Methods Phys. Res.* B **358** 160
[39] Zweit J *et al* 1987 *Int. J. Radiat. Appl. Instrum.* A **38** 499